Desalination and Water Treatment
www.deswater.com

doi: 10.5004/dwt.2022.28869

273 (2022) 64–72
October

High-performance filtration PAN-based electrospun nanofibers membranes with hierarchical structure for oil separation

Haneen S. Al-Okaidy, Basma I. Waisi*

Department of Chemical Engineering, College of Engineering, University of Baghdad, Iraq, email: basmawaisi@coeng.uobaghdad.edu.iq (B.I. Waisi) ORCID ID: 0000-0001-7842-5541; email: haneen.mohammad1607@coeng.uobaghdad.edu.iq (H.S. Al-Okaidy) ORCID ID: 0000-0001-9099-0738

Received 14 April 2022; Accepted 21 August 2022

ABSTRACT

Nanofibers-based membranes are essential separation membranes due to their several advantages for oil-water separation. However, the low mechanical strength is the weak point of nanofibers membranes due to their small fiber diameters, extremely porous structure, and insufficient fiber bonding. This study fabricated a multilayers configuration of polyacrylonitrile (PAN) electrospun nanofibers membrane of a hierarchical structure by electrospinning three solutions of different PAN concentrations (10, 13, and 16 wt.%) consequently. Then, the solvent-vapor method was used as a post-treatment modification approach to improve the mechanical properties of the fabricated PAN-based multilayers nanofibers membrane via solvent-induced fusion of inter-fiber junction points. The surface morphology, fibers size, porosity, and mechanical properties were investigated to evaluate the modification effect on the fabricated membranes. According to the analysis results, the post-treated multilayers PAN-based nanofibers membranes significantly enhanced their strength and flexibility. In addition, the fabricated membranes were applied in emulsified oil filtration using a cross-flow cell filtration system. The post-treated multilayers PAN-based membrane by vapor-solvent showed a high performance with a long operating time.

Keywords: Nanofibers; Multilayers; Emulsified oil; Crossflow cell; Filtration

1. Introduction

As a result of the rapid growth in global energy demand, numerous oil contamination accidents have occurred during offshore oil production and transportation procedures [1]. Most industrial wastewater contains emulsified oil (droplet size less than 20 μm) among its pollutants [2,3]. At the moment, oil-water separation technologies fall into three categories: chemical processes (flocculation and dispersant), biological processes, and physical processes (flotation, skimming, and filtration) [4,5]. However, oil removal remains a global engineering difficulty because of the various phase states of oil, the small size of the oil droplets (less than 10 μm), and the comparatively high viscosity [6]. Membrane filtration technology has garnered considerable interest in water purification treatment because of its integrity, low energy consumption, simple performance, and friendliness to the environment [1,7,8].

Electrospinning has long been regarded as an extraordinarily robust and versatile method for producing nanofibrous materials from a polymeric solution under a high voltage field [1,9]. It is a valuable and uncomplicated way to produce customized surfaces with submicron to nanoscale fibers that are becoming increasingly common [10]. The electrospinning method is characterized by the ease with which additives can be combined in nanofibers, the high versatility that enables precise control of nanofiber diameter, membranes with porosity of more than 90%, and high surface-to-volume ratio [11,12]. Owing to their unique

* Corresponding author.

properties, the nanofibers membranes were preferred choices to be used in various applications such as drug delivery systems [13], protective clothing [14], solar cells [15], lithium-ion batteries [16], sensors [17], and air filtration [18,19]. Despite the inherent advantages of nanofibers filtration membranes, they are generally avoided in wastewater treatment due to their low mechanical strength due to their small fiber diameters, extremely porous structure, and insufficient fiber bonding [1,20].

Several methods have been developed to provide suitable mechanical strength to electrospun nanofibers. One of these methods is to fabricate dual or multilayers membranes. It is well documented that the membrane support layer provides mechanical strength and significantly affects the permeability of composite membranes [21]. The developed dual layers or multilayer structured membranes combine several distinct advantages of individual layers to address the problem [6,22]. For water filtration, composite membranes with multi-layer composite structures have been developed to reduce membrane resistance and enhance permeate flux [23]. Yoon et al. [24] fabricated three-tier composite membranes by a direct spinning of polyacrylonitrile (PAN)/dimethylformamide (DMF) solution onto the surface-coated PET non-woven substrate.

The other approach is improving the bonding of nanofibers at the junction points in the nanofiber membranes using a solvent vapor or by controlling the solvent composition of the electrospinning solution [25,26]. By this method, the fibers weld, and the connection points reinforce using a minimally invasive post-treatment procedure that does not materially alter the membrane's morphology or dimensions. This post-treatment involves using solvent vapor that may stay on the fibers in their nonwoven structure after spinning. This solvent will aid in fusing fibers at junctions [27]. Huang and her group applied the DMF solvent vapor post-treatment strategy to modify the mechanical strength of the fabricated 10% PAN/DMF-based nanofiber membrane that contained uniform fibers, as they produced using one concentration of polymer [28].

In this work, the mechanical property of the membranes was enhanced by the emerging two strategies. First, fabricating PAN-based nanofibers membrane with a hierarchical structure by spinning multilayers of various PAN/DMF concentrations (10, 13, and 16 wt.%) spun consequently within the same membrane mat. Then, the fabricated membrane was exposed to DMF vapor post-treatment method for various time. Combining these two strategies is supposed to show a better modification of the membrane strength because of the different effect of the solvent vapor on the various fiber sizes. The joint points containing small fibers can be effected and melt more than the large fibers, increasing the flexibility of the membrane. Meanwhile, the large fibers in the membrane are important to increase the strength of the fibers at the breakpoints. By this way, the mechanical strength of the fabricated membrane of different fiber sizes would be modified better than membranes that contain the uniform sizes of fibers. The surface morphology, porosity, and mechanical strength were assessed using the analysis devices. Additionally, the resilience of the fabricated nanofibers membrane's high mechanical pressure was evaluated using a cross-flow cell in oil filtration.

2. Materials and methods

2.1. Electrospinning of nanofibers membranes

The polymer polyacrylonitrile (PAN) (molecular weight = 150,000 g/mol) and the solvent N,N-dimethylformamide (DMF) (density = 0.948 g/cm^3) were purchased from Aldrich and Alfa Aesar, respectively. To obtain transparent solutions of PAN/DMF of different concentrations (10, 13, and 16 wt.%), a specific amount of PAN was dissolved in DMF at 50°C for 5 h of stirring. All the nanofibers membranes in this work were created using the electrospinning approach, which includes the pulling action of polymer droplets in a high voltage 22–24 kV electrostatic field. The setup of the basic electrospinning contains a syringe containing a polymer solution, a needle made of metal, a voltage power supply, also a collector [29].

The single-layer PAN-based membrane configuration was prepared by spinning the 10% PAN/DMF solution on the collector to fabricate. The Multilayer configuration membrane with a hierarchical structure was prepared by spinning the various PAN solution concentrations (10%, 13%, and 16%) layer by layer.

All the fibers were spun at the same process parameters; the distance between the needle and collector of 15 cm, the injection flow rate of 1 mL/h, and the speed of the collector speed of 140 rpm. All the fabricated membranes were fabricated at room temperature at humidity (10–20). All the fabricated membranes had a thickness of 200–250 μm.

2.2. Post-treatment by solvent vapor

To enhance the mechanical strength of the multilayer PAN-based nanofibers membranes, the PAN-based nanofibers membranes were, immediately after fabrication, sealed in a glass desiccator saturated with DMF vapor for 4 d and then air-dried for 24 h to evaporate the residual DMF solvent before further characterization.

2.3. Emulsion preparation

To prepare the feed solution of 300 mg/L concentration of emulsion solution (oil/water), a specific amount of Kerosene (from midland Iraqi refineries company) was added to distilled water and mixed using the ultrasonic processor (Hielscher UP400s, Teltow, Germany) at 10,000 rpm for 20 min at room temperature. The oil concentration in water was measured using a UV/V spectrophotometer; the wavelength was 196 nm.

2.4. Membrane characterizations

The surface morphology of the multilayer PAN-based nonwoven electrospun nanofibers (before and after treatment with the vapor-solvent of DMF solvent) was observed using a scanning electron microscope (SEM, JEOL6335F). From each sample, the diameter of 35 fibers were measured using the Image-J software to evaluate the diameter distribution. Also, the organic fouling on the fabricated membranes was conceived by comparing the SEM images of the surface morphology of the fabricated nanofibers membranes before and after emulsified oil removal from water.

The porosity of a membrane is critical for various membrane applications, most notably the separation performance of membranes. To assess the porosity of ENMs membranes, weighed a sample of each membrane prior to immersing it in distilled water for 1 h. The weight of the sample was determined before and after immersion in water as dry and wet weights, respectively. The porosity percentage of the nanofibers membranes was then calculated using Eq. (1) [30]:

$$\text{Porosity}(\%) = \frac{(W_1 - W_2)}{A \cdot t \cdot \rho} \quad (1)$$

where W_1 and W_2 are wet and dry membrane mass (g), A is membrane area (cm^2), t is membrane thickness (cm), and ρ: water density at room temperature g/cm^3.

The membrane's mechanical strength is critical for practical applications such as reusability, handling, and deformation resistance [31]. The mechanical properties of the membranes were obtained using a dynamic mechanical analyzer (DMA) by measuring the breaking strength and Young's modulus of the membrane samples (AG-A10T, Shimadzu, Japan). Young's modulus, which indicates an elastic material's rigidity, can be described as the stress-to-strain ratio [32]. Flexible materials have a low Young's modulus. The tests were conducted at a temperature of 25°C using a specimen with a length of 10 cm and a width of 1 cm.

2.5. Emulsified oil filtration experiments

Fig. 1 shows the schematic diagram of the used cross-flow filtration system for emulsified oil removal from synthetic oily wastewater. The filtration system contained a homemade cross-flow filtration cell, a vessel for feed solution, a feed pump, and a pressure gauge. The size of the made cross-flow filtration cell was 14 cm^3 × 5 cm^3 × 3 cm^3. The dimensions of the electrospun nanofiber membrane that would be cut were 2 cm × 10 cm and put in the membrane cell. First of all, the operation of the filtration system was run with distilled water for the first 20 min to settle down the flux through the membrane. Then, oil/water emulsion was fed to be filtered through the membrane cell. The operating conditions of the filtration experiments were 300 mg/L inlets emulsified oil concentration, 70 mL/min feed flow rate, 25 psig transmembrane pressure, and 25°C temperature. The performance of the fabricated modified and unmodified multilayer PAN-based nonwoven nanofiber membranes (permeate flux and oil rejection) were investigated under different transmembrane pressures to evaluate the DMF vapor-modification effect on the mechanical properties of the PAN-based single-layer and multilayer nanofibers membranes.

The flux of the membrane (J) (LMH) and the percentage of the oil rejection (R) (%) in operating running time was calculated using the equations, respectively [33]:

$$J = \frac{V}{At} \quad (2)$$

$$R\% = \left(1 - \frac{C_t}{C_o}\right) \times 100 \quad (3)$$

where the volume of permeate flow is V (L), A (m^2) is the effective area of the membrane, and the filtration time is presented by t (h). The initial oil concentration in the feed is C_o (mg/L), and C_t (mg/L) at any time.

3. Results and discussion

3.1. Membrane characterizations

3.1.1. Influence of membrane configuration

Fig. 2 presents the SEM images of the top surface and the corresponding fiber size distribution of the two fabricated membranes configurations: single layer and multilayers PAN-based nanofibers membranes. Fig. 2a shows that spinning a single layer of 10% PAN/DMF produced straight, continuous, beads-free, and homogeneous fibers. Most of the produced fibers fall in the 200–300 nm range, with an average size of 290 nm.

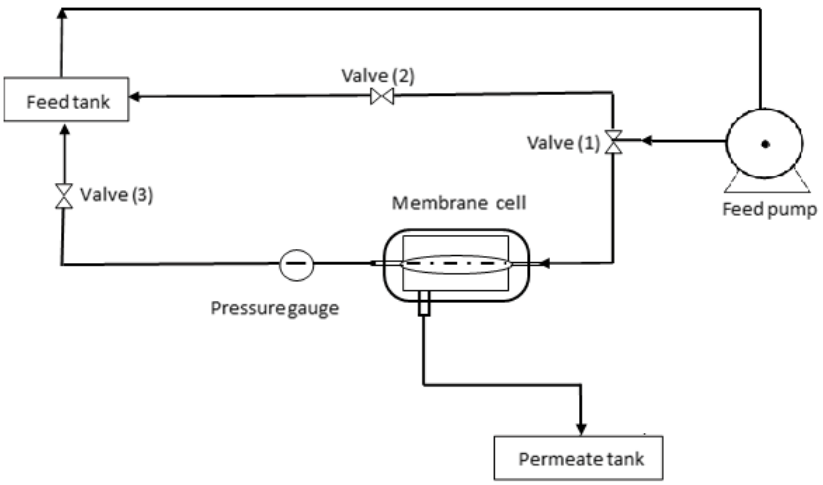

Fig. 1. Schematic diagram of the cross-flow filtration system.

Fig. 2b shows the fabricated multilayer PAN-based membrane's surface morphology from spinning various concentrations (10, 13, and 16 wt.%) of PAN/DMF layer by layer. The SEM images of the multilayer configuration showed that the fabricated fibers had a wide range of diameters due to different PAN concentrations in the spinning process. It is well known that the fiber diameter increases with the concentration of the polymeric solution due to increasing the viscosity of the spinning solution, which reduces the drawdown of the fiber prior to solidification [34]. Thus, the fiber size distribution of the fabricated multilayers membrane was wide and mainly distributed between 200 to 500 nm producing an average fiber size of 360 nm.

The values of porosity, tensile strength, and Young's modulus of the two configurations of PAN-based nanofibers membranes are presented in Table 1. Compared to a single layer 10% PAN-based nanofibers membrane, the multilayers of various concentrations (10%, 13%, 16%) PAN solution resulted in a slight increase in the porosity due to the large fiber sizes of the produced configuration. Also, the multilayer configuration showed higher tensile strength and flexibility, attributed to the included large fibers of the high polymer concentration. Spinning a high concentration polymeric solution produces more polymer chains per fiber and causes increasing chain interaction and entanglement. Larger fibers also contain a more residual

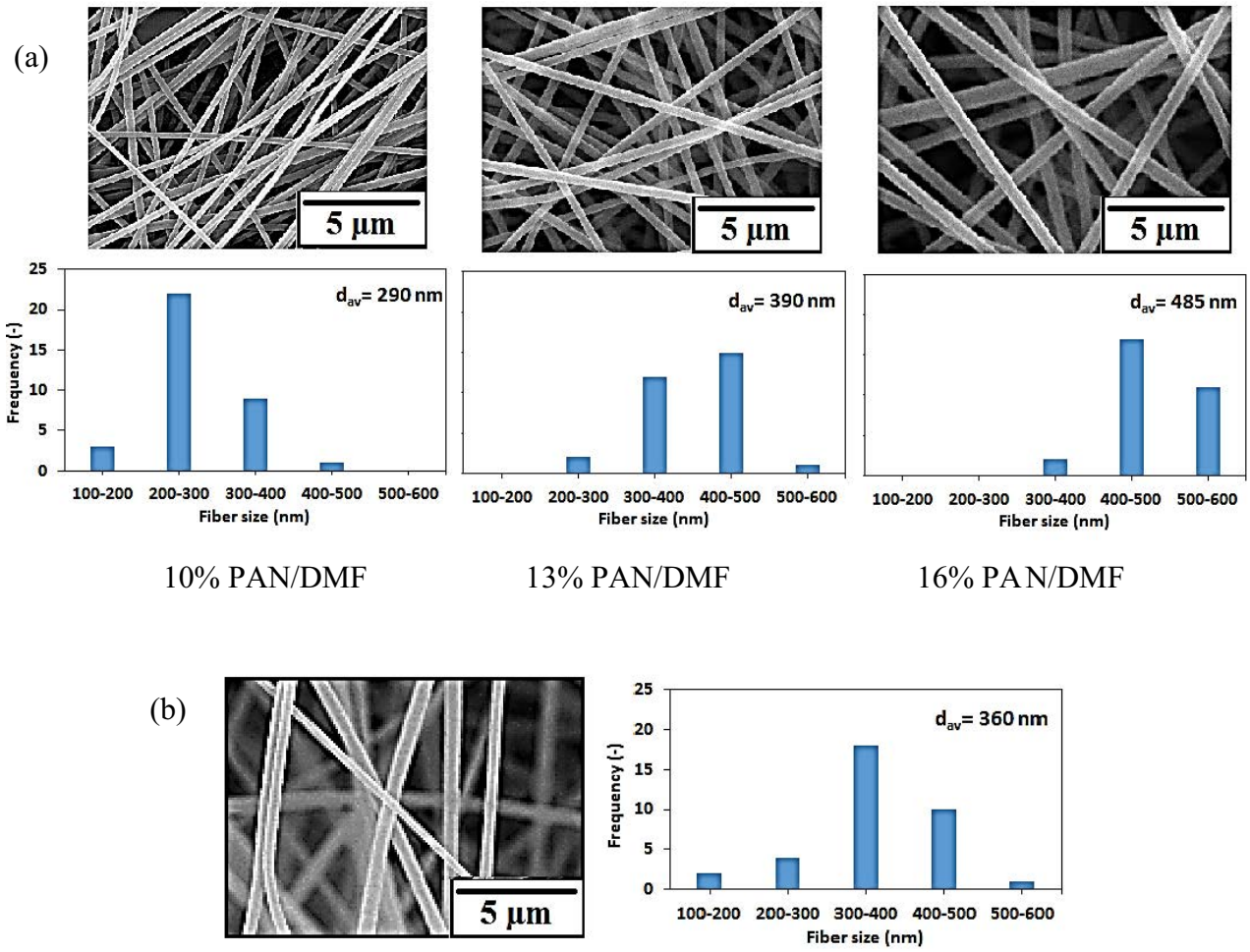

Fig. 2. The SEM images and the corresponded fiber size distribution of the fabricated PAN-based nanofibers membrane (a) single-layer configuration and (b) multilayers configuration.

Table 1
Characterizations of the two fabricated configurations of PAN-based nanofibers membranes

Configuration of nanofiber membranes	Average fiber size (nm)	Porosity (%)	Tensile stress (MPa)	Young's modulus (MPa)
Single layer 10% PAN-based membrane	290 ± 5	94 ± 1	1.4	16
Multilayer (10, 13, and 16 wt.%) PAN-based membrane	360 ± 8	95 ± 1	2.2	9.23

solvent in their core than smaller fibers. The solvent evaporation facilitates the bonding of fibers; thus, the strength of the membrane improves [34].

3.1.2. Influence of solvent vapor treatment

Fig. 3 illustrates SEM images of the post-treated single layer and multilayers PAN-based nanofibers membranes by exposing them to DMF vapor for 4 d. The surface morphology of both post-treated configurations showed significant change compared to the untreated fibers shown in Fig. 2. The effect of exposing a membrane of uniform fibers size (single layer membrane) for DMF vapor is different from that of a membrane that includes different sizes of fibers (the multi-layers membrane). In the single-layer membrane, the impact of DMF vapor is the same on all fibers. However, in the multilayers membranes, some of the small fibers might melt in the conjunction points while the large fibers might swell, increasing the membrane strength in several aspects.

In the fiber size distribution of the single-layer membrane in Fig. 3a, PAN-based fibers appeared to swell, increasing the size of the fibers to the range of 300–400 nm. Fig. 3b indicated that all the fibers in the multilayers membranes swelled to a larger size and increased the average fiber size to 420 nm. Swelling the PAN-based fibers is related to the high polymer-solvent affinity. Also, it has been noticed from the corresponded fiber sizes that the small fibers were mainly affected by the solvent vapor than the large fibers, which could be related to the higher penetration of solvent in the small fibers. Also, the SEM images showed that fusion occurred among most fiber junctions due to condensing the solvent at the junction points and slightly dissolving the polymer to facilitate fusion [20].

Table 2 presents the porosity, tensile strength, and Young's modulus values of the post-treated two configurations of PAN-based nanofibers membranes. Exposing the fabricated nanofibers membranes to solvent vapor did not affect the porosity value. However, the mechanical strength of the membranes increased after the post-treatment step.

Generally, the strength and Young's modulus of the fabricated PAN-based fibers membrane improved due to swelling the fibers and solvent-induced fusion at the fiber junction points, as seen in the SEM images. Also,

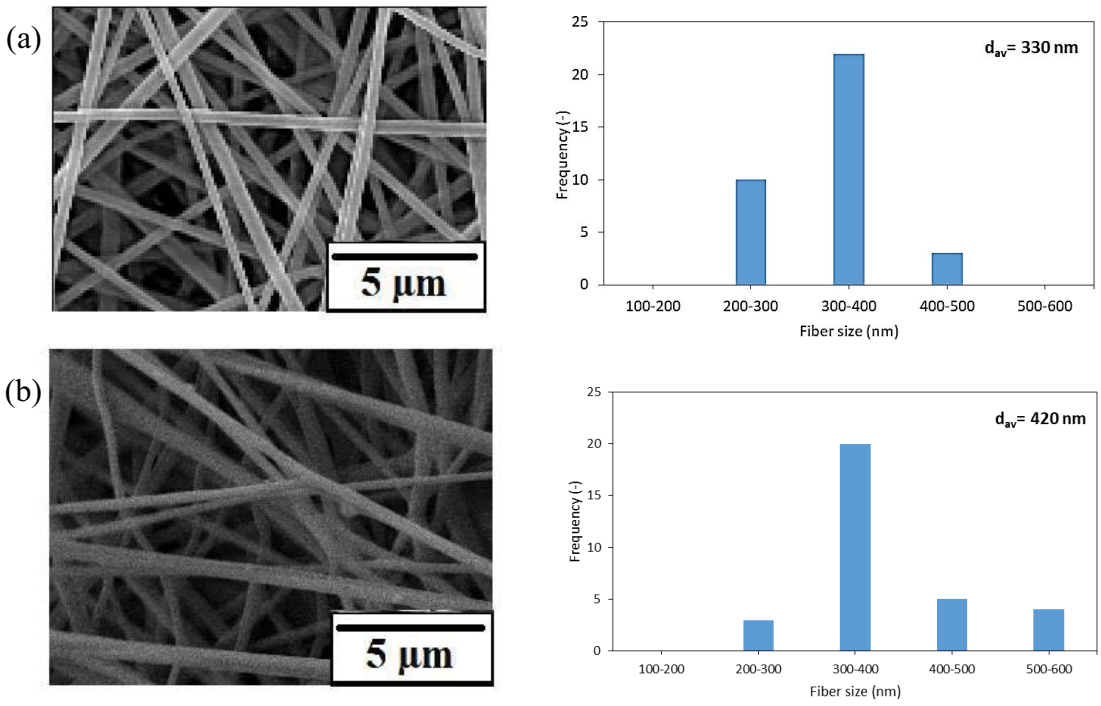

Fig. 3. The SEM images and the corresponded fiber size distribution of the post-treated PAN-based nanofibers membrane (a) single-layer configuration and (b) multilayers configuration.

Table 2
Characterizations of the post-treated two configurations of PAN-based nanofibers membranes

Post-treated nanofiber membranes	Average fiber size (nm)	Porosity (%)	Tensile stress (MPa)	Young's modulus (MPa)
Single layer 10% PAN-based nanofiber membrane	330 ± 6	94 ± 1	2	19
Multilayers (10%, 13%, 16%) PAN-based nanofiber membrane	420 ± 9	92 ± 1	2.44	11.3

the improvement in the fiber strength of single layer 10% PAN-based membrane (1.4–2 MPa) was more than that in multilayer configuration membrane (2.2 to 2.44 MPa), which can be attributed to the homogenously of the fiber sizes. The number of small fibers in the single layer of 10% PAN-based fibers membranes is more than that in the multilayer configuration; thus, the junction points fused during the post-treatment are more.

3.2. Membrane performance in filtration

3.2.1. Effect of membrane configuration

The performance of the two fabricated configurations (single and multilayers) of PAN-based membranes has been investigated in emulsified oil removal from water using a cross-flow filtration system. The permeate flux and oil rejection percentage for the fabricated membranes over the experiment time are shown in Fig. 4a and b under a transmembrane pressure of 25 psig. Regarding the single layer, 10% PAN-based nanofiber membrane, the permeate flux was reasonable at 13000 LMH due to the high porosity. Over time, the permeate flux declined to 5000 LMH at the rupture time (45 min) due to the accumulated oil droplets on the membrane surface clogged the permeate flux passages. Also, the oil rejection increased from 80% to 93% at the rupture time, which is attributed to the effect of the excluded emulsified oil droplets size that decreased the pore diameter of the membranes. On the other hand, the multilayer configuration showed less oil rejection percentage than the single-layer membrane because of the large fibers and pores within its structure, while the rupture time was more than 2 h.

Fig. 5 presents the formed fouling on the fabricated membrane surfaces at the rupture time. The fouling was coalescences of excluded oil droplets during attempts at moving through the mats. The amount of fouling on the surface of the multilayer configuration (Fig. 5b) was much more than that formed on the single-layer membrane (Fig. 5a), which is attributed to the longer experiment time till the membrane ruptured.

According to the above results, incorporating layers of large fibers of 13% and 16% PAN/DMF on the top side of the small fibers of 10% PAN/DMF layer to fabricate the configuration of the multilayer resulted in decreasing the oil rejection but also increased the membrane strength and withstand longer time till rupture point.

3.2.2. Effect of solvent vapor treatment

To investigate the effect of vapor post-treatment on the membrane performance, the treated membranes were used for oil filtration using a cross-flow filtration system and compared with the performance of the untreated

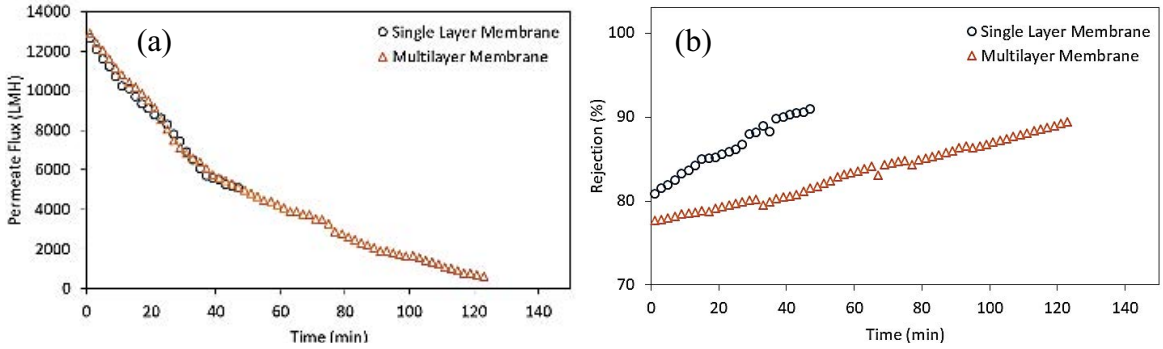

Fig. 4. The oil/water filtration efficiency using the two fabricated configurations: single-layer and multilayers nanofibers membranes (a) permeate flux and (b) oil rejection percentage.

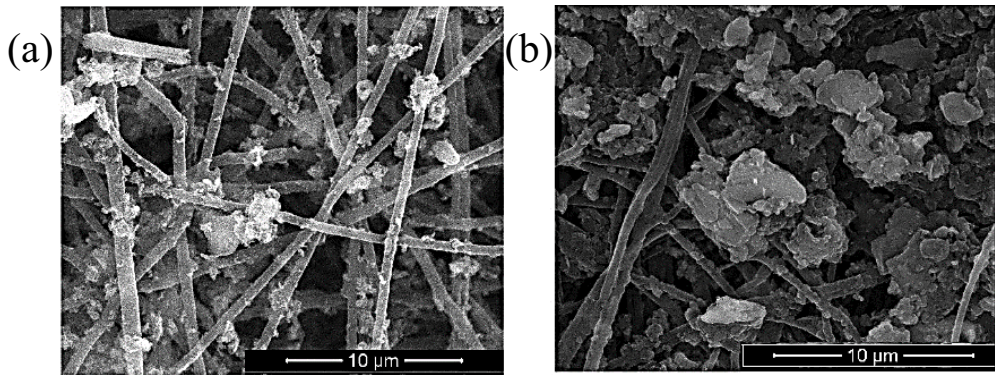

Fig. 5. The SEM images of the two fabricated configurations after the oil filtration process (a) single-layer and (b) multilayers nanofibers membranes.

membranes. Fig. 6a and b present the filtration performance of the untreated and treated single membranes. The early fiber rupture due to the low mechanical strength of membranes is the disadvantage of 10% PAN-based nanofibers membrane. Post treating of 10% PAN-based nanofibers membrane enhanced fiber strength (as shown in Tables 1 and 2) and tripled the filtration time. Thus the treated membrane could be used in oil filtration for a longer time.

The untreated and treated multilayers configuration performances are shown in Fig. 7a and b. the results indicated that the post-treating the fabricated multilayer configuration membrane treated increased the filtration time and the oil rejection. This result is attributed to the obvious increase in the fibers' size and strength (as shown in Tables 1 and 2). The permeate flux of the post-treated multilayers membrane was more than the untreated membrane, which can be attributed to the effect of DMF vapor on the structure of the fiber. The number of large fibers in the treated multilayers membrane is more than that in the untreated membranes because of the swelling of the fibers during the post-treatment step. The large fibers played an important role in excluding the big droplets of emulsified oil, while the rest of the oil droplets were removed by the small fibers leading to a high rejection of oil with no

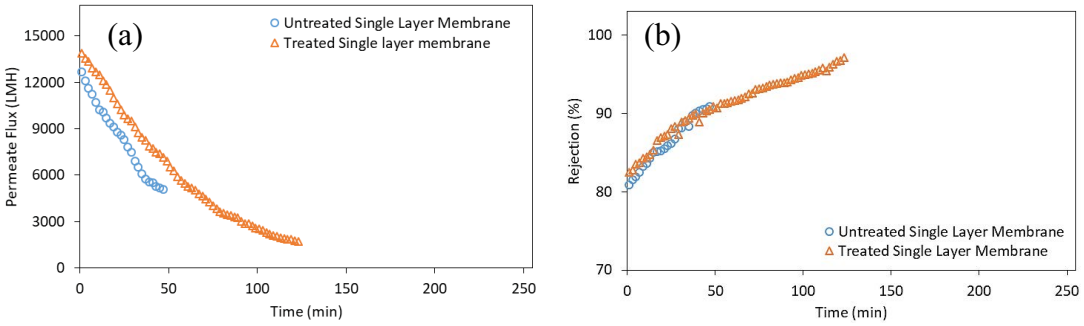

Fig. 6. The oil filtration performance comparison of the untreated and post-treated single-layer nanofibers membranes (a) permeate flux and (b) oil rejection percentage.

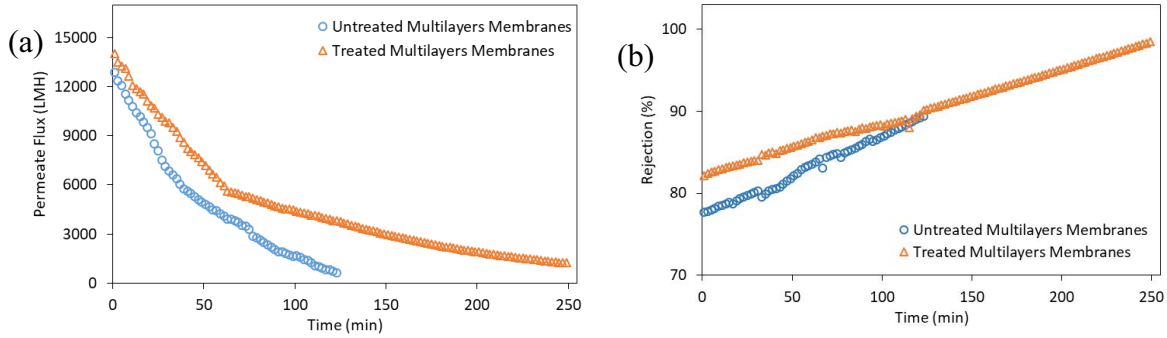

Fig. 7. The oil filtration performance comparison of the untreated and post-treated multilayer nanofibers membranes (a) permeate flux and (b) oil rejection percentage.

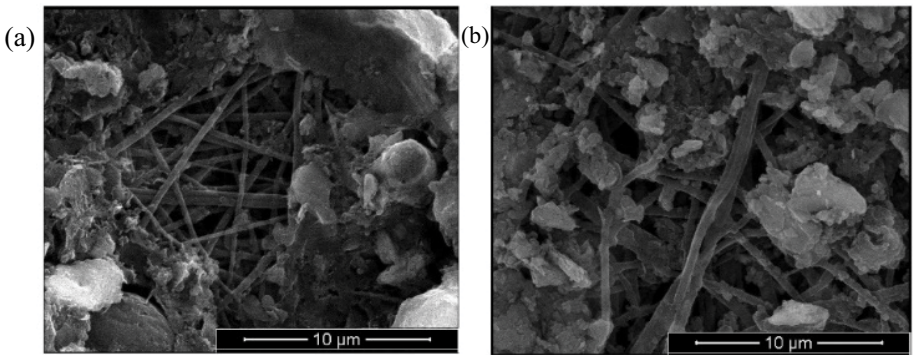

Fig. 8. The SEM images of the post-treated PAN-based nanofibers membranes after the oil filtration process (a) single-layer configuration and (b) multilayer configuration.

slow accumulation of oil fouling amongst the small fibers of the membrane. As a result, the permeate flux through the treated multilayer membrane was higher than in the untreated membrane due to the slow accumulation of oil fouling. Also, the filtration time (till membrane rupturing) of the post-treated multilayers configuration membrane was twice that of the untreated multilayers membranes reaching up to more than 4 h indicating the membrane's strength improvement

Fig. 8 presents the formed fouling on the surface of the post-treated membranes at the rupture time. The excluded oil droplets on the treated multilayer membrane (Fig. 8b) were more than on the treated single-layer membrane (Fig. 8a) due to the longer filtration time. According to the above results, incorporating layers of large fibers of 13% and 16% PAN/DMF on the top side of the small fibers of 10% PAN/DMF layer to fabricate the configuration of the multilayer resulted in decreasing the oil rejection but also increased the membrane strength and withstand longer time till rupture point.

In addition, the performance of the most improved nanofiber membrane (post-treated multilayer membrane) was evaluated under higher transmembrane pressure, and it was found that the TMP was 35 psig using pure water flow through the filtration cell.

4. Conclusion

Electrospun nanofibers have dragged great attention in the filtration of oil/water mixtures for their high surface-to-volume ratio. Highly porous nanofibers structures can be produced by electrospinning a polymeric solution; however, the low mechanical strength is the main disadvantage of this membrane type. In this study, two approaches were applied to enhance the nanofibers membrane's mechanical strength and filtration performance.

The first method was fabricating nanofibers membrane with hierarchical structure by spinning various concentrations of 10%, 13%, and 16% PAN/DMF solutions layer by layer, producing a configuration of multilayer nanofibers membranes. Compared with 10% PAN/DMF single-layer polymeric membranes, the multilayer nanofibers membrane showed higher strength than the single-layer membrane; thus, it could operate in oil filtration for a longer operating time. For more improvement in the mechanical properties of the multilayer nanofibers membranes, the post-treatment by solvent vapor for 4 d showed significant improvement in the membrane strength. The fabricated membranes were applied for oil filtration using a cross-flow filtration system to investigate the effect of the applied modification on the membrane filtration performance. The results showed better permeate flux and oil rejection with longer operating filtration time, up to six times for 10% PAN/DMF nanofibers membrane.

The obtained results showed a significant enhancement in the treated multilayer configuration membranes' mechanical properties without affecting membrane flux and rejection performance. Thus, the treated multilayer nanofibers membrane operates in the oil filtration system for a longer time, up to six times than that for 10% PAN/DMF nanofibers membrane. Also, the treated multilayer nanofibers membrane could withstand TMP of 35 psig in a cross-flow filtration cell. The followed enhancement procedure in this work showed a good strength improvement compared with other complicated procedures.

References

[1] X. Yue, Z. Li, T. Zhang, D. Yang, F. Qiu, Design and fabrication of superwetting fiber-based membranes for oil/water separation applications, Chem. Eng. J., 364 (2019) 292–309.

[2] B.I.H. Waisi, U.F.A. Karim, D.C.M. Augustijn, M.H.O. Al-Furaiji, S.J.M.H. Hulscher, A study on the quantities and potential use of produced water in southern Iraq, Water Sci. Technol. Water Supply, 15 (2015) 370–376.

[3] M.L. Hassan, S.M. Fadel, R.E. Abouzeid, W.S. Abou Elseoud, E.A. Hassan, L. Berglund, K. Oksman, Water purification ultrafiltration membranes using nanofibers from unbleached and bleached rice straw, Sci. Rep., 10 (2020) 11278, doi: 10.1038/s41598-020-67909-3.

[4] J. Ge, H.-Y. Zhao, H.-W. Zhu, J. Huang, L.-A. Shi, S.-H. Yu, Advanced sorbents for oil-spill cleanup: recent advances and future perspectives, Adv. Mater., 28 (2016) 10459–10490.

[5] I.F. Guha, K.K. Varanasi, Low-voltage surface electrocoalescence enabled by high-K dielectrics and surfactant bilayers for oil–water separation, ACS Appl. Mater. Interfaces, 11 (2019) 34812–34818.

[6] J. Ge, Q. Jin, D. Zong, J. Yu, B. Ding, Biomimetic multilayer nanofibrous membranes with elaborated superwettability for effective purification of emulsified oily wastewater, ACS Appl. Mater. Interfaces, 10 (2018) 16183–16192.

[7] R.W. Field, Surface science: separation by reconfiguration, Nature, 489 (2012) 41–42.

[8] S.M. Seyed Shahabadi, J.A. Brant, Bio-inspired superhydrophobic and superoleophilic nanofibrous membranes for non-aqueous solvent and oil separation from water, Sep. Purif. Technol., 210 (2019) 587–599.

[9] B.I. Waisi, Carbonized copolymers nonwoven nanofibers composite: surface morphology and fibers orientation, Iraqi J. Chem. Pet. Eng., 20 (2019) 11–15.

[10] R.S. Barhate, S. Ramakrishna, Nanofibrous filtering media: filtration problems and solutions from tiny materials, J. Membr. Sci., 296 (2007) 1–8.

[11] Y. Liao, C.-H. Loh, M. Tian, R. Wang, A.G. Fane, Progress in electrospun polymeric nanofibrous membranes for water treatment: fabrication, modification and applications, Prog. Polym. Sci., 77 (2018) 69–94.

[12] M. Barani, S. Bazgir, M. Keyvan Hosseini, P. Keyvan Hosseini, Eco-facile application of electrospun nanofibers to the oil-water emulsion separation via coalescing filtration in pilot-scale and beyond, Process Saf. Environ. Prot., 148 (2021) 342–357.

[13] T.J. Sill, H.A. von Recum, Electrospinning: Applications in drug delivery and tissue engineering, Biomaterials, 29 (2008) 1989–2006.

[14] B. Yoon, S. Lee, Designing waterproof breathable materials based on electrospun nanofibers and assessing the performance characteristics, Fibers Polym., 12 (2011) 57–64.

[15] X.G. Zhao, E.M. Jin, J.-Y. Park, H.-B. Gu, Hybrid polymer electrolyte composite with SiO_2 nanofiber filler for solid-state dye-sensitized solar cells, Compos. Sci. Technol., 103 (2014) 100–105.

[16] H. Aydın, S.Ü. Çelik, A. Bozkurt, Electrolyte loaded hexagonal boron nitride/polyacrylonitrile nanofibers for lithium ion battery application, Solid State Ionics, 309 (2017) 71–76.

[17] A. Macagnano, V. Perri, E. Zampetti, A. Bearzotti, F. De Cesare, F. Sprovieri, N. Pirrone, A smart nanofibrous material for adsorbing and detecting elemental mercury in air, Atmos. Chem. Phys., 17 (2017) 6883–6893.

[18] Z. Li, W. Kang, H. Zhao, M. Hu, N. Wei, J. Qiu, B. Cheng, A novel polyvinylidene fluoride tree-like nanofiber membrane for microfiltration, Nanomaterials, 6 (2016) 152, doi: 10.3390/nano6080152.

[19] Y. Liao, M. Tian, R. Wang, A high-performance and robust membrane with switchable super-wettability for oil/water separation under ultralow pressure, J. Membr. Sci., 543 (2017) 123–132.
[20] L. Huang, S.S. Manickam, J.R. McCutcheon, Increasing strength of electrospun nanofiber membranes for water filtration using solvent vapor, J. Membr. Sci., 436 (2013) 213–220.
[21] M. Al-Furaiji, J.T. Arena, J. Ren, N. Benes, A. Nijmeijer, J.R. McCutcheon, Triple-layer nanofiber membranes for treating high salinity brines using direct contact membrane distillation, Membranes (Basel), 9 (2019) 60, doi: 10.3390/membranes9050060.
[22] S. Ling, Z. Qin, W. Huang, S. Cao, D.L. Kaplan, M.J. Buehler, Design and function of biomimetic multilayer water purification membranes, Sci. Adv., 3 (2017) 1–12, doi: 10.1126/sciadv.1601939.
[23] X. Wang, K. Zhang, Y. Yang, L. Wang, Z. Zhou, M. Zhu, B.S. Hsiao, B. Chu, Development of hydrophilic barrier layer on nanofibrous substrate as composite membrane via a facile route, J. Membr. Sci., 356 (2010) 110–116.
[24] K. Yoon, K. Kim, X. Wang, D. Fang, B.S. Hsiao, B. Chu, High flux ultrafiltration membranes based on electrospun nanofibrous PAN scaffolds and chitosan coating, Polymer, 47 (2006) 2434–2441.
[25] D. Haas, S. Heinrich, P. Greil, Solvent control of cellulose acetate nanofibre felt structure produced by electrospinning, J. Mater. Sci., 45 (2010) 1299–1306.
[26] C. Liu, X. Li, T. Liu, Z. Liu, N. Li, Y. Zhang, C. Xiao, X. Feng, Microporous CA/PVDF membranes based on electrospun nanofibers with controlled crosslinking induced by solvent vapor, J. Membr. Sci., 512 (2016) 1–12.
[27] I. Erukhimovich, M.O. de la Cruz, Phase equilibria and charge fractionation in polydisperse polyelectrolyte solutions, J. Polym. Sci., Part B: Polym. Phys., 45 (2004) 2288–2300.
[28] L. Huang, J.T. Arena, S.S. Manickam, X. Jiang, B.G. Willis, J.R. McCutcheon, Improved mechanical properties and hydrophilicity of electrospun nanofiber membranes for filtration applications by dopamine modification, J. Membr. Sci., 460 (2014) 241–249.
[29] M. Al-Furaiji, M. Kadhom, K. Kalash, B. Waisi, N. Albayati, Preparation of thin-film composite membranes supported with electrospun nanofibers for desalination by forward osmosis, Drinking Water Eng. Sci., 13 (2020) 51–57.
[30] S.M. Alkarbouly, B.I. Waisi, Fabrication of electrospun nanofibers membrane for emulsified oil removal from oily wastewater, Baghdad Sci. J., 19 (2022) 1238, doi: 10.21123/bsj.2022.6421.
[31] N. Naseeb, A.A. Mohammed, T. Laoui, Z. Khan, A novel PAN-GO-SiO_2 hybrid membrane for separating oil and water from emulsified mixture, Materials (Basel), 12 (2019) 212, doi: 10.3390/ma12020212.
[32] M. Rabiei, A. Palevicius, A. Dashti, S. Nasiri, A. Monshi, A. Vilkauskas, G. Janusas, Measurement modulus of elasticity related to the atomic density of planes in unit cell of crystal lattices, Materials (Basel), 13 (2020) 4380, doi: 10.3390/ma13194380.
[33] Q. Wang, J. Cui, S. Liu, J. Gao, J. Lang, C. Li, Y.Yan, Facile preparation of halloysite nanotube-modified polyvinylidene fluoride composite membranes for highly efficient oil/water emulsion separation, J. Mater. Sci., 54 (2019) 8332–8345.
[34] B.I. Waisi, S.S. Manickam, N.E. Benes, A. Nijmeijer, J.R. McCutcheon, Activated carbon nanofiber nonwovens: improving strength and surface area by tuning fabrication procedure, Ind. Eng. Chem. Res., 58 (2019) 4084–4089.